Light-induced transcriptional responses associated with proteorhodopsin-enhanced growth in a marine flavobacterium

Hiroyuki Kimura[1,3], Curtis R. Young[1], Asuncion Martinez[1] and Edward F. DeLong[1,2]

[1]Department of Civil and Environmental Engineering, Massachusetts Institute of Technology, Cambridge, MA 02139, USA
[2]Department of Biological Engineering, Massachusetts Institute of Technology, Cambridge, MA 02139, USA
[3]Department of Geosciences, Faculty of Science, Shizuoka University, Shizuoka, Shizuoka 422-8529, Japan

*Correspondence: Edward F. DeLong
Department of Civil and Environmental Engineering, Massachusetts Institute of Technology, Parsons Laboratory 48-427, 15 Vassar Street, Cambridge, MA 02139, USA.
E-mail: delong@mit.edu
Tel: (617) 253-0252

Running title: Transcriptomics of PR-containing flavobacterium
Keywords: Flavobacteria/marine/photoheterotrophy/proteorhodopsin/transcriptomics
Subject Category: Integrated genomics and post-genomics approaches in microbial ecology

ABSTRACT: Proteorhodopsin (PR) is a photoprotein that functions as a light-driven proton pump in diverse marine Bacteria and Archaea. Recent studies have suggested that PR may enhance both growth rate and yield in some flavobacteria when grown under nutrient limiting conditions in the light. The direct involvement of PR, and the metabolic details enabling light-stimulated growth however, remain uncertain. Here, we surveyed transcriptional and growth responses of a PR-containing marine flavobacterium during carbon-limited growth in the light and the dark. As previously reported (Gómez-Consarnau *et al*., Nature 445: 210-213, 2007), *Dokdonia* strain MED134 exhibited light-enhanced growth rates and cell yields under low carbon growth conditions. Inhibition of retinal biosynthesis abolished the light-stimulated growth response, supporting a direct role for retinal-bound PR in light enhanced growth. Among protein-coding transcripts, both PR and retinal biosynthetic enzymes showed significant upregulation in the light. Other light-associated proteins, including bacterial cryptochrome and DNA photolyase, were also expressed at significantly higher levels in the light. Membrane transporters for Na^+/phosphate and Na^+/alanine symporters, and the Na^+-translocating NADH-quinone oxidoreductase (NQR) linked electron transport chain, were also significantly upregulated in the light. Culture experiments using a specific inhibitor of Na^+-translocating NQR indicated that sodium pumping via NQR is a critical metabolic process in the light-stimulated growth of MED134. In total, the results suggested the importance of both the PR-enabled, light-driven proton gradient, as well as the generation of a Na^+ ion gradient, as essential components for light-enhanced growth in these flavobacteria.

Introduction

Some prokaryotes possess proteins that interact with light, and convert it into energy for growth or into sensory information. One class of energy-harvesting photoproteins called rhodopsins consist of single, membrane-embedded protein covalently bound to the chromophore retinal (a light-sensitive pigment) (Spudich and Jung, 2005). Ten years ago, prokaryotic rhodopsin, proteorhodopsin (PR), was discovered through metagenomic analyses of marine bacterioplankton genome fragments (reviewed by DeLong and Béjà, 2010). Béjà *et al.* (2000) found that an uncultivated marine SAR86 clade member in Gammaproteobacteria contained a bacteriorhodopsin-like gene, dubbed PR. Further, the marine SAR86-derived PR functioned as a proton pump, when the recombinant *Escherichia coli* expressing PR is exposed to light. PRs were subsequently detected in many other marine bacteria, some of which appeared to be "tuned" to absorb specific wavelengths of light associated with their habitat of origin; green light in surface waters and blue light in deep waters (Béjà *et al*., 2001). Additional studies have found PR genes in a diverse array of abundant marine bacterial and archaeal clades (Giovannoni *et al*., 2005; Frigaard *et al*., 2006; Brown and Jung, 2006; McCarren and DeLong, 2007). Based on genomic surveys, a large fraction of naturally occurring marine bacterioplankton in oceanic surface seawaters appear to contain the PR gene (de la Torre *et al*., 2003; Sabehi *et al.*, 2005; Moran and Miller, 2007; DeLong 2009). Interestingly, chromophore biosynthetic genes including a carotenoid biosynthetic gene cluster, and a novel blh gene encoding a 15,15'-β-carotene dioxygenase that cleaves β-carotene to yield retinal, were found linked to the PR gene in some microorganisms (Sabehi *et al.*, 2005). Martinez *et al.* (2007) demonstrated that the expression of the entire PR photosystem (genetically linked PR and retinal biosynthetic genes) in *E. coli* can result in proton-pumping activity in light, and that the resulting pmf can be used for ATP synthesis via the membrane-embedded ATP synthase. Furthermore, PR in

recombinant *E. coli* can generate a light-driven pmf sufficient to increase the rate of flagellar rotation, providing estimates for energy flux through the photosystem (Walter *et al*., 2007).

PR-containing marine bacterial isolates have been recently cultured from a variety of marine environments. These isolates include members of SAR11 (Alphaproteobacteria), OM43 (Betaproteobacteria), and SAR 92 (Gammaproteobacteria) clades, as well as members of the Bacteroidetes and Vibrionaceae (Giovannoni *et al*., 2005; Frigaard *et al*., 2006; McCarren and DeLong, 2007; Stingl *et al*., 2007; González *et al*., 2008). Laboratory experiments examining light-stimulated growth in some of these isolates however have proven equivocal. Some studies could detect no significant light enhancement of either growth rates or cell yields in PR-containing isolates (Giovannoni *et al*., 2005; Stingl *et al.*, 2007). However, light-enhanced growth rates and cell yields were reported in one PR-containing marine flavobacterium, *Dokdonia* sp. MED134 (Gómez-Consarnau *et al*., 2007). Additionally, microcosm studies suggested that some of marine flavobacteria and SAR11 populations exhibited enhanced expression of the PR gene in the presence of light (Lami *et al*., 2009). As well, Gómez-Consarnau *et al*. (2010) demonstrated the enhanced long-term survival of PR-containing *Vibrio* cells in the light, but not in darkness. Nevertheless, the specific metabolic processes that facilitate light-enhanced growth or survival are not yet well understood.

To better characterize the photophysiology of PR-containing Flavobacteria, we performed transcriptomic analyses targeting total RNA extracted from MED134 exposed to light or in the dark. Transcriptional profiles derived from cultures incubated in the light and dark were analyzed, and these results were used to further direct laboratory experiments using different growth substrates and inhibitors. The effect of light on growth at various carbon concentrations, and the effect of retinal biosynthesis inhibitors on light-enhanced growth, were explored. In addition, the effects of sodium-translocating respiratory chain

inhibitors on light-stimulated on growth were also examined. The combined results from both gene expression studies and physiological experiments were used to develop a model that incorporates some of the important features of photoheterotrophic growth observed in *Dokdonia* strain MED 134.

Materials and methods

Strain and culture conditions

PR-containing marine flavobacterium, *Dokdonia* sp. MED134, was isolated from surface seawater in Northwest Mediterranean Sea (Gómez-Consarnau *et al*., 2007). This strain was kindly provided to us by Jarone Pinhassi (University of Kalmar, Sweden). MED134 was grown in artificial seawater (ASW) (35 practical salinity units, prepared from Sea Salts; Sigma) containing low concentration of dissolved organic carbon (DOC) (0.05 mM C). ASW was filter-sterilized through 0.2 µm-pore-size filter system (Nalgene) and autoclaved. Then 250 ml aliquots of ASW (containing a background concentration of 0.05 mM C of DOC), were partially supplemented with full strength medium (FSM; 0.5 g of peptone [Bacto Pepton, BD] and 0.1 g of yeast extract [Bacto Yeast Extract, BD] per 100 ml of ASW), to yield final DOC concentrations of 0.14 and 0.39 mM C, respectively. All media were also supplemented with 225 µM of NH_4Cl and 44.7 µM of $Na_2HPO_4 \cdot 12H_2O$, to avoid inorganic nitrogen and phosphate limitation. DOC concentrations were measured using the high temperature combustion method on TOC-V (Shimadzu) with platinized aluminum catalyst. The bacteria were initially grown in ASW enriched to 1.1 mM C, washed in ASW, and then diluted into three different ASW media, each containing a different DOC concentration (0.05, 0.14 and 0.39 mM C). Cultures were incubated at 22ºC under continuous white light (approximately 150 µmol of photons m^{-2} s^{-1}) or in the darkness.

To determine bacterial cell density, cultures were filtered with pre-blackened Isopore membrane filter (pore size, 0.22 μm; Millipore). Bacterial cells on the filter were stained with SYBR Green I (1:100 dilution; Molecular Probes) for 15 min, and counted under an epifluorescence microscope (Axioskop 2, Zeizz). All culture experiments were performed in triplicate.

Cultivation for transcriptomic analyses

MED134 was grown on 900 ml of ASW enriched to 0.14 mM C at 22ºC in the darkness for the first 2 days. At this time, 400 ml of culture was filtered onto a pore-size 0.22-μm Durapore membrane filter (25 mm diameter, Millipore), yielding the D2 sample. The remaining culture was split in two 250 ml flasks that were incubated again at 22ºC under the continuous white light (approximately 150 μmol of photons m^{-2} s^{-1}) or in the darkness. After 2 more days, the cultures were filtered onto Durapore membrane filters (Millipore), yielding samples L2 (light conditions) and D4 (dark conditions), respectively. Filter samples were immediately placed into screw-cap tubes containing 1 ml of RNAlater (Ambion) and stored at -80ºC until RNA extraction.

Total RNA extraction and rRNA subtraction

Total RNA was extracted from the filter samples using a modification of the *mir*Vana miRNA isolation kit (Ambion) as described previously (Shi *et al*., 2009; McCarren *et al*., 2010). Briefly, filter samples were thawed on ice, and the RNAlater surrounding each filter was removed and discarded. The filters were immersed in Lysis/Binding buffer (Ambion) and mixed to lyse attached cells. Total RNA was extracted from the lysate according to the manufacturer's protocol. Remaining genomic DNA in RNA extraction was removed using a TURBO DNA-free kit (Ambion).

Bulk DNA was extracted from MED134 cultured under suitable condition based on a conventional extraction protocol. Cells of strain were lysed with lysozyme and proteinase K solution. Then the genomic DNAs were extracted with phenol-chloroform-isoamyl alcohol and precipitated with ethanol.

16S and 23S rRNAs were removed by the subtractive hybridization described by Stewart *et al.* (2010). Ribonucleotide probes targeting 16S and 23S rRNA genes were generated from the bulk DNA extracted from MED134. Templates for probe generation were first prepared by PCR using Herculase II Fusion DNA Polymerase (Stratagene) and strain-specific primers flanking nearly the full length of the bacterial 16S and 23S rRNA genes, with reverse primers modified to contain the T7 RNA polymerase promoter sequence (Supplementary Table S1). Biotinylated antisense rRNA probes were generated by *in vitro* transcription with T7 RNA polymerase, ATP, GTP, CTP, UTP, biotin-11-CTP, biotin-16-UTP (Roche). Biotinylated rRNA probes were hybridized to complimentary rRNA molecules in total RNA sample. Then biotinylated double-stranded rRNA was removed from the sample by hybridization to Streptavidin-coated magnetic beads (New England Biolabs). The subtraction efficiency was evaluated by monitoring the removal of 16S and 23S peaks from total RNA profiles using a 2100 Bioanalyzer (Agilent).

RNA amplification, cDNA synthesis, and pyrosequencing

The rRNA-subtracted RNA (10-15 ng) was amplified using the MessageAmp II-Bacteria kit (Ambion) as described previously (Shi *et al*., 2009; McCarren *et al*., 2010). In brief, total RNA were polyadenylated using *Escherichia coli* poly(A) polymerase. Polyadenylated RNA was converted to double-stranded cDNA via reverse transcription primed with an oligo(dT) primer containing a promoter sequence for T7 RNA polymerase and a recognition site for the restriction enzyme *Bpm*I (T7-*Bpm*I-$(dT)_{16}$VN) (Supplementary Table S1). cDNA was

transcribed *in vitro* at 37°C for 12 hr, yielding large quantities (40-60 μg) of single-stranded antisense RNA. The SuperScript double-stranded cDNA synthesis kit (Invitrogen) was used to convert antisense RNA to double-stranded cDNA, which was then digested with *Bpm*I to remove poly(A) tails. Prior to pyrosequencing, poly(A)-removed cDNA was purified by using the AMPure kit (Beckman Coulter Genomics). Purified cDNA was used for the generation of single-stranded DNA libraries and the bead-bound fragments were amplified by emulsion PCR according to established protocols (454 Life Sciences, Roche). The resulting bead-bound single stranded cDNAs were then pyrosequenced on the 454 FLX platform (Roche). All the cDNA sequences generated in this study have been submitted to the GenBank short read archive under accession number SRA029329.

Analyses of pyrosequence data

rRNA and tRNA reads were identified using BLASTN against rRNA and tRNA sequences in MED134 genome data, which are deposited in GenBank under accession no. AAMZ00000000 (Gómez-Consarnau *et al*., 2007). Reads producing alignments with bit scores greater than 50 were considered as rRNA and tRNA sequences. Protein-encoding cDNAs (from mRNA) were identified using BLASTX against peptide sequences collected from MED134 genome data (bit score ≥50). Small RNAs (sRNAs) were analyzed using the Rfam (version 10.0) website (http://rfam.sanger.ac.uk/). Rfam is a collection of non-coding RNA families, each represented by multiple sequence alignments, consensus secondary structures, and covariance models, including 1,446 families in January 2010 (Gardner *et al.*, 2009). Finally, in order to identify MED134 specific sRNA that might not be represented in Rfam, we assembled a database of intergenic regions (IGRs) in the genome of MED134 longer than 100 bp (total 992 sequences) which might encode putative sRNAs. Reads with matches to the IGRs database (bit score ≥50) were considered sRNA reads.

L2/D4 ratios were calculated based on read number of each cDNA, which was normalized by total number of protein-encoding reads in each sample. The statistic significance of the change observed between cultures in light and dark (L2 and D4) for each cDNA was determined based on false-discovery rate method (q-value ≤ 0.05) (Benjamini and Hochberg, 1995; Storey and Tibshirani, 2003). Clustering analyses of transcriptomics datasets were performed in GenePattern (Reich *et al*., 2006), using hierarchical clustering (Eisen *et al*., 1998) by Pearson correlations for both rows and columns, using pairwise complete-linkage.

Culture experiments with specific inhibitors

To confirm an importance of retinal-bound PR for the light-stimulated growth, we performed culture experiments with 2-(4-methylphenoxy)triethylamine hydrochloride (MPTA). MPTA is known to prevent lycopene cyclization in retinal biosynthesis pathway (Cunningham *et al*., 1994; Armstrong, 1999). First, we cultured MED134 on Marine Agar 2216 (Difco) amended with MPTA at a final concentration of 300 µM and confirmed the effect of MPTA against strain MED134 based on color of colonies. Next, MED134 was grown in ASW slightly enriched with FSM (0.14 mM C) and amended with MPTA. MPTA was dissolved in methanol and added to ASW at a final concentration of 100 µM. The same volume of methanol was added to cultures as negative control without MPTA. These cultures were incubated at 22ºC under continuous white light (approximately 150 µmol of photons m^{-2} s^{-1}) or in the darkness. The cultures were performed in triplicate. Bacterial cell density was measured every 2 days by the direct counting method with epifluorescence microscope described above. Additionally, colony-forming unit (cfu) was also monitored after spread 100 µl of cultures on Marine Agar 2216 (Difco) and incubation at 22ºC for 48 hr. MPTA was a generous gift of Francis X. (Buddy) Cunningham (University of Maryland, USA).

227 To determine the importance of sodium pumping in light-driven growth of PR-
228 containing marine flavobacteria, MED134 was grown in ASW with 2-*n*-heptyl-4-
229 hydroxyquinoline *N*-oxide (HQNO) (Enzo Life Sciences). HQNO is known to be a specific
230 inhibitor of the electron-transport-linked Na^+-translocating NQR enzyme complex (Tokuda
231 and Unemoto, 1982; Häse and Mekalanos, 1999). MED134 was incubated in ASW enriched
232 with DL-alanine (0.70 mM C), supplemented with trace element solution (Futamata *et al.*,
233 2009), and amended with HQNO at a final concentration of 10 µM. DL-alanine was selected
234 as carbon source for the bacterial cultivation, since transcriptomic analyses demonstrated
235 significant over representation of Na^+/alanine symporters in the presence of light (see Results
236 and discussion). HQNO was prepared in ethanol. The same volume of ethanol was added to
237 culture as negative control without HQNO. These cultures were incubated at 22ºC under
238 continuous white light or in the dark. The cultures were performed in triplicate. Bacterial
239 cell densities were measured every 2 days by the direct count and plate count method
240 described above.
241
242

243 ## Results and discussion

244 *Cultivation in light and darkness*

245 *Dokdonia* sp. MED134 exposed to light reached a maximal abundance of 1.1×10^5 cell ml^{-1}
246 in unamended artificial seawater (ASW) (DOC, 0.05 mM C), 1.4×10^6 cell ml^{-1} in ASW
247 enriched with 0.14 mM C, and 1.1×10^7 cell ml^{-1} in ASW enriched to 0.39 mM C (Figure 1).
248 In contrast, dark-incubated cultures remained below 5.0×10^4 cells ml^{-1} in unenriched ASW.
249 In nutrient enriched ASW media, MED134 grew moderately in the dark, but the cell yields
250 were much lower compared to cultures grown in the light. Light/dark ratios of cell yields
251 ranged from 1.6 to 4.6 at the peak of the growth curves. Growth rates in ASW containing

252 0.14 mM C were 0.69 day^{-1} in the illuminated culture (logarithmic growth phase, 1.5 to 5
253 day), and 0.44 day^{-1} in the dark cultures (logarithmic growth phase, 1.5 to 4 day). Growth
254 rates in ASW containing 0.39 mM C were 1.17 day^{-1} in the light, and 1.01 day^{-1} in the dark
255 (logarithmic growth phase, 0 to 4 day). These results show the considerable influence of PR
256 on growth rate at low carbon concentrations, and its lesser influence at higher carbon
257 concentrations. These findings confirm the previous work of Gómez-Consarnau *et al.*
258 (2007), which showed that light has a definite positive impact on the growth of the PR-
259 containing flavobacteria grown in low carbon conditions.
260
261 *Transcriptome experiments*
262 For transcriptomic analyses, MED134 was grown again in ASW enriched to 0.14 mM C.
263 Bacteria grew to 1.0×10^5 cells ml^{-1} for first 2 days in the dark (D2). After 2 more days,
264 MED134 reached 3.2×10^5 cells ml^{-1} in light (L2), whereas bacteria incubated in darkness
265 remained 1.2×10^5 cells ml^{-1} (D4).
266 cDNAs synthesized from the RNA samples were pyrosequenced on the Roche 454
267 FLX platform, yielding ≈400,000 reads per sample. cDNA derived from intergenic regions
268 (IGRs) accounted for 21 to 51% of the total cDNA reads (Figure 2). Remarkably, most of
269 reads derived from IGRs in all samples corresponded to a single gene (399 bp) encoding
270 transfer-messenger RNA (tmRNA) (Supplementary Table S2). tmRNA is small RNA that
271 employs both tRNA-like and mRNA-like properties as it rescues stalled ribosomes during
272 nutrient shortage (Gillet and Felden, 2001; Keiler, 2008; Moore and Sauer, 2007). Since the
273 proportions of tmRNA further increased with incubation time, the high percentage of tmRNA
274 is likely to be due to the carbon limiting growth conditions used in this experiment. Protein-
275 encoding transcripts, identified by comparison with the annotated MED134 genome
276 (GenBank version in December 2009), represented 38 to 61% of total cDNA reads (Figure

277 2). Genes with a significant change in L2/D4 ratio (q-value ≤0.05) were considered
278 differentially expressed in the light versus the dark. Using this criteria, 601 genes in 2,944
279 annotated protein-encoding genes were found to be differentially expressed. Specifically,
280 312 genes were upregulated in the light, whereas 289 genes exhibited downregulation in the
281 light.
282
283 *PR and retinal biosynthetic enzymes*
284 Previous genomic analysis of MED134 revealed the presence of genes encoding PR, and
285 *crtEBIY* encoding enzymes needed to synthesize β-carotene from farnesyl diphosphate (FPP)
286 (Gómez-Consarnau *et al*., 2007). Further, a gene (*blh*) encoding an enzyme that converts β-
287 carotene to retinal has been also found next to the PR gene on the genome of MED134. Our
288 transcriptomic survey revealed that the L2/D4 ratios for the PR gene, *crtEBIY* and *blh* were
289 elevated (Figure 3a). In particular, statistical significance tests based on q-values showed that
290 the PR, *crtE* and *crtI* genes were significantly upregulated in the culture exposed to light
291 (Table 1). In addition, hierarchical clustering of transcript abundances clustered D2 and D4
292 together, to the exclusion of L2 (Figure 3b). This clustering pattern reflects the differential
293 response of this PR-containing flavobacterium to light. Gómez-Consarnau *et al*. (2007)
294 demonstrated by RT-PCR that MED134 had a higher expression of PR gene in the light than
295 in the dark. Lami *et al.* (2009) also reported that marine flavobacteria and SAR11 in natural
296 costal seawaters displayed significant high expression of PR gene in the presence of light.
297 Our results extend these previous reports and indicate that transcription of the entire PR
298 photosystem is upregulated in the presence of light in this flavobacterium.
299 The only evidence supporting the role of PR in light-stimulated growth in strain
300 MED134 is the observation that only light corresponding to the wavelengths absorbed by PR
301 elicited growth enhancement (Gómez-Consarnau *et al*., 2007). To better define the role of

PR in light-stimulated growth in strain MED134, we performed culture experiments with MPTA, a specific inhibitor of lycopene cyclization in the retinal biosynthetic pathway (Cunningham *et al.*, 1994; Armstrong, 1999; see Figure 3a). First, MED134 was grown on agar plates enriched with peptone and yeast extracts with and without MPTA. In the presence of MPTA, MED134 produced light pink colonies, whereas yellow colonies were observed on agar plates without MPTA (Figures 4a and 4b). In general, it is known that bacterial cells accumulating β-carotene display yellow or orange colonies, whereas light pink colonies indicate accumulation of lycopene (Cunningham *et al.*, 1994; Armstrong, 1999). Our results indicate that MPTA effectively prevented β-carotene generation, the precursor for retinal, in strain MED134. MED134 was grown in ASW enriched to 0.14 mM C and amended with MPTA. When strain MED134 was incubated in ASW with MPTA, bacteria grew moderately to 6.3×10^5 cells ml^{-1} and 4.3×10^5 cfu ml^{-1} in the presence of light (Figures 4c and 4d). In contrast, MED134 incubated in ASW without MPTA in the light produced significantly higher yields (1.9×10^6 cells ml^{-1} and 1.5×10^6 cfu ml^{-1}) than those in ASW with MPTA. In culture experiments in the dark with or without MPTA, bacteria grew similarly to approximately 5.0×10^5 cells ml^{-1} (3.0×10^5 cfu ml^{-1}), equivalent to the results with MPTA in the light. The findings suggest that PR bound to retinal plays a critical role in the light-stimulated growth of the PR-containing marine flavobacteria.

ATP synthetase

The genome of MED134 harbors genes encoding membrane-embedded ATP synthetase, a multi-unit enzyme consisting of two large complexes. In this study, large numbers of transcripts from ATP synthetase were identified, however, there was no significant difference in ATP synthetase transcript abundance in the light and dark cultures (Supplementary Table S3).

Light sensors

MED134 contains several gene homologs of membrane sensors known to respond to light. González *et al.* (2008) reported that MED134 contain genes encoding bacterial cryptochrome and several DNA photolyase/cryptochromes that belong to different gene families (DASH family, (6-4) photolyase family, and class I photolyase). Similar genes encoding these light sensor proteins were also identified in the genome sequence of *Polaribacter* sp. MED152, another marine flavobacterium (González *et al.*, 2008). Further, MED134 has PAS and GAF domains, known to be common components of phytochromes that detect red and far-red light (Taylor and Zhulin, 1999; Anantharaman *et al.*, 2001). PAS domains are able to respond to oxygen levels, redox potential and light, whereas GAF domains work as phototransducers. Another gene associated with light sensing contains the BLUF domain, which specifically responds to blue light (Gomelsky and Klug, 2002). The BLUF domain is also found in the genome of related *Polaribacter* sp. MED152 (González *et al.*, 2008). In addition to light sensors, several histidine (His) kinases, which might play important roles for secondary transduction and response regulation, are contained in the genome of MED134.

In this study, we found significant upregulation of bacterial cryptochrome and two putative DNA photolyase/cryptochrome genes under light (L2) versus dark (D4) conditions (Table 2). In contrast, genes encoding PAS, GAF, and BLUF domains exhibited no significant difference between light and dark cultures (Supplementary Figure S1). Of the secondary transduction enzymes, one His kinase (MED134_10396) showed very high expression rate (L2/D2 ratio, 18.3) and significant upregulation in light (Table 2). This His kinase may therefore be involved in controlling gene expression in response to light.

Central metabolic pathways

352 The main energy generating metabolic pathways of MED134 identified by genome analyses
353 were glycolysis, the pentose phosphate cycle, and the TCA cycle (Gómez-Consarnau *et al*.,
354 2007). Several genes encoding enzymes working in the central metabolic pathways were
355 significantly induced in culture exposed to light (Supplementary Table S4). In particular,
356 genes encoding fructose-bisphosphatase (*fbp*) in glycolysis, glucoce-6-phosphate
357 dehydrogenase (*zwf*) and phosphogluconate dehydrogenase (*gnd*) in pentose phosphate cycle,
358 and succinate dehydrogenase (*sdhABC*) and fumarate hydratase (*fumC*) in TCA cycle
359 exhibited significant upregulation in light. In addition, hierarchical clustering of transcript
360 abundances clustered D2 and L2 together, to the exclusion of D4 (Supplementary Figure S2).
361 This clustering pattern may reflect the increased levels of carbon available in the D2 culture,
362 and the additional energy source (light) available in the L2 culture, relative to the D4 culture.
363 Hence, the expression pattern of enzymes of the central metabolic pathways may reflect the
364 differential nutrient and energy availability between the different treatments.
365 MED134 also harbors genes encoding pyruvate carboxylase (*pycA*) and
366 phosphoenolpyruvate (PEP) carboxylase (*ppc*) that function in anaplerotic metabolism and
367 that are associated with carbon fixation (González *et al*., 2008). Pyruvate carboxylase
368 generates oxaloacetate from bicarbonate and pyruvate, whereas PEP carboxylase synthesizes
369 oxaloacetate from bicarbonate and PEP (Attwood and Wallace, 2002; Izui *et al*., 2004;
370 Jitrapakdee *et al*., 2008). The transcript abundance of pyruvate carboxylase and PEP
371 carboxylase were significantly downregulated in the light, compared to that in the dark
372 (Supplementary Table S5). In contrast, SulP-type bicarbonate transporter and carbonic
373 anhydrase, which is known to interconvert CO_2 and bicarbonate, were not significant
374 different between L2 and D4. Although *Polaribacter* sp. MED152 has been reported to fix
375 more bicarbonate in the light than in the darkness (González *et al*., 2008), our findings
376 indicate that in MED134 CO_2 incorporation via pyruvate carboxylase and PEP carboxylase

377 may be equally important for anaplerotic carbon replenishment under both dark and light
378 growth conditions.
379
380 *Transporters and electron transport chain*
381 Membrane transporters play critical roles in uptake of essential nutrients and minerals. The
382 genome of MED134 contains relatively low numbers of genes encoding membrane
383 transporters, compared to other marine bacteria. Transcriptomic analyses revealed that two
384 predicted Na^+/alanine symporters (MED134_02355, MED134_14567) were significantly
385 upregulated in the light (Table 1 and Supplementary Figure S3). Further, a Na^+/phosphate
386 symporter (MED134_11180) also exhibited significant upregulation in the light.
387 Transcriptome analyses also indicated significant upregulation of Na^+-translocating NQR,
388 succinate dehydrogenase, and cytochrome c oxidase in the light (Table 1 and Supplementary
389 Figure S4). These results suggested the potential importance of the sodium ion gradient for
390 transport fractions in the light, and the potential of indirect light-stimulation of sodium pump
391 activities via the light-driven proton gradient (see Supplementary Figure S5).
392 To test the importance of sodium ion exchange in light-stimulated physiology of
393 MED134, we performed growth experiments with HQNO, a specific inhibitor of Na^+-
394 translocating NQR (Tokuda and Unemoto, 1982; Häse and Mekalanos, 1999). MED134 was
395 grown in ASW amended with and without HQNO. For these experiments, DL-alanine was
396 chosen as carbon source, because of the high expression levels of Na^+/alanine symporter we
397 observed in cultures grown in the light. In cultures without HQNO, MED134 increased to
398 2.6×10^5 cells ml^{-1} (2.3×10^5 cfu ml^{-1}) in the light and 1.3×10^5 cells ml^{-1} (1.1×10^5 cfu ml^{-1}) in the dark (Figure 5) when grown on DL-alanine. Cell yields in cultures incubated with
400 HQNO in the light were about 3 times less than those grown in the absence of inhibitor. In
401 contrast, for cultures grown in the dark, cell yields decreased by about 1/2 in the presence of

the inhibitor, although the amount of growth on DL alanine was much lower. These findings indicate that the Na^+-translocating NQR may play a critical role in sodium pumping in light-stimulated growth, and that active PR photophysiology greatly enhances the ability of these flavobacteria to grow on DL alanine.

Conclusion

In this study, we characterized gene expression patterns associated with the higher growth rates and cell yields observed in flavobacterium strain MED134 in carbon-limited media, when grown in the light. Among protein-encoding transcripts, a number of genes were upregulated in the light, including PR, retinal biosynthetic enzymes, and several predicted light sensors (Figure 6). Previous studies had suggested the involvement of PR in light enhanced growth, because the action spectra for this response generally matched the PR absorption spectrum. Experiments with MPTA, a specific inhibitor of an enzyme in retinal biosynthetic pathway, confirmed the involvement of PR in the observed light-enhanced growth. MED134 cultures grown with MPTA exhibited much lower cell yields than those without MPTA, when both were grown in the presence of light, while MPTA had no effect on MED134 grown in the dark. Proteins involved in some central metabolic pathways, including fructose-bisphosphatase, glucoce-6-phosphate dehydrogenase, phosphogluconate dehydrogenase, succinate dehydrogenase, and fumarate hydratase, also had relatively higher expression in light than dark, suggesting an increased requirement for these enzymes during active cell growth. Transcripts for membrane embedded ATP synthase, and pyruvate carboxylase and PEP carboxylase were well represented in both the light and dark grown cultures. These results likely reflect a central and essential requirement for ATP synthetase and the two carboxylases, in both the light and the dark.

Of the membrane transporters, Na^+/phosphate symporter and Na^+/alanine symporter exhibited particularly significant upregulation in cultures exposed to light. The Na^+-translocating NQR linked electron transport chain also exhibited significantly greater expression levels in the light. The gene expression levels of other sodium pumps however, including the Na^+/H^+ antiporter and the Na^+ efflux pump, did not appear significantly different between the L2 and D4 treatments (Figure 6). These results indicate the potential importance of these symporters, coupled with the central role of NQR in driving energy-requiring nutrient transport via its maintenance of the sodium ion gradient. Culture experiments using a specific inhibitor of Na^+-translocating NQR, HQNO, also suggested the importance of the sodium ion gradient for MED134 growth, and indicated that sodium pumping via Na^+-translocating NQR is critical metabolic process for the light-stimulated growth of PR-containing marine flavobacteria, in addition to proton pumping via retinal-bound PR. In total, our findings indicate a direct role for retinal-bound PR in light-enhanced growth in *Dokdonia* strain MED134. Furthermore, an important role for H^+/Na^+ ion exchange, and transport processes that utilize energy derived from the sodium ion gradient, appear particularly important for the photoheterotrophic growth in this flavobacterium strain.

Acknowledgements

We thank Jarone Pinhassi for providing strain MED134 and Francis X. (Buddy) Cunningham for providing MPTA. We are also grateful to Jamie W. Becker for measuring DOC in media, Frank J. Stewart for helping with the rRNA subtraction, Yanmei Shi for helping small RNA analyses, and Rachel Barry for work in preparing samples for pyrosequencing. This work was supported by a grant from the Gordon and Betty Moore Foundation (EFD), the Office of Science (BER), U.S. Department of Energy (EFD), and NSF Science and Technology Center Award EF0424599. This work is a contribution of the Center for Microbial Oceanography: Research and Education (C-MORE). H. Kimura was supported by Postdoctoral Fellowships for Research Abroad of Japan Society for the Promotion of Science (JSPS).

References

Anantharaman V, Koonin EV, Aravind L. (2001). Regulatory potential, phyletic distribution and evolution of ancient, intracellular small-molecule-binding domains. *J Mol Biol* **307:** 1271–1292.

Armstrong G. (1999). Carotenoid genetics and biochemistry. In: Cane DE (ed). *Isoprenoids including carotenoids and steroids*. Vol. 2. Elsevier: Amsterdam, Netherlands. pp 321-352.

Attwood PV, Wallace JC. (2002). Chemical and catalytic mechanisms of carboxyl transfer reactions in biotin-dependent enzymes. *Acc Chem Res* **35:** 113–120.

Béjà O, Aravind L, Koonin EV, Suzuki MT, Hadd A, Nguyen LP, Jovanovich SB, Gates CM, Feldman RA, Spudich JL, Spudich EN, DeLong EF. (2000). Bacterial rhodopsin: evidence for a new type of phototrophy in the sea. *Science* **289:** 1902-1906.

Béjà O, Spudich EN, Spudich JL, Leclerc M, DeLong EF. (2001). Proteorhodopsin phototrophy in the ocean. *Nature* **411:** 786-789.

Benjamini Y, Hochberg Y. (1995). Controlling the false discovery rate: a practical and powerful approach to multiple testing. *J R Statist Soc B* **57:** 289-300.

Brown LS, Jung K-H. (2006). Bacteriorhodopsin-like proteins of eubacteria and fungi: the extent of conservation of the haloarchaeal proton-pumping mechanism. *Photochem Photobiol Sci* **5:** 538-546.

Cunningham FX, Sun Z, Chamovitz D, Hirschberg J, Gantt E. (1994). Molecular Structure and Enzymatic Function of Lycopene Cyclase from the Cyanobacterium *Synechococcus* sp Strain PCC7942. *Plant Cell* **6:** 1107-1121.

de la Torre JR, Christianson LM, Béjà O, Suzuki MT, Karl DM, Heidelberg J, DeLong EF. (2003). Proteorhodopsin genes are distributed among divergent marine bacterial taxa. *Proc Natl Acad Sci USA* **100:** 12830-12835.

DeLong EF. (2009). The microbial ocean from genomes to biomes. *Nature* **459:** 200-206.

DeLong EF, Béjà O. (2010). Light-driven proton pump proteorhodopsin enhances bacterial survival during tough times. *PLoS Biol* **8:** e1000359. doi:10.1371/journal.pbio.1000359

Eisen MB, Spellman PT, Brown PO, Botstein D. (1998). Cluster analysis and display of genome-wide expression patterns. *Proc Natl Acad Sci USA* **95:** 14863-14868.

Frigaard N-U, Martinez A, Mincer TJ, DeLong EF. (2006). Proteorhodopsin lateral gene transfer between marine planktonic Bacteria and Archaea. *Nature* **439:** 847-850.

485 Futamata H, Kaiya S, Sugawara M, Hiraishi A. (2009) Phylogenetic and transcriptional
486 analyses of a tetrachloroethene-dechlorinating "*Dehalococcoides*" enrichment culture
487 TUT2264 and its reductive-dehalogenase genes. *Microbes Environ* **24:** 330-337.
488 Gardner PP, Daub J, Tate JG, Nawrocki EP, Kolbe DL, Lindgreen S *et al*. (2009). Rfam:
489 updates to the RNA families database. *Nucleic Acids Res* **37:** D136-D140.
490 Gillet R, Felden B. (2001). Emerging views on tmRNA-mediated protein tagging and
491 ribosome rescue. *Mol Microbiol* **42:** 879–885.
492 Giovannoni SJ, Bibbs L, Cho J-C, Stapels MD, Desiderio R, Vergin KL *et al*. (2005).
493 Proteorhodopsin in the ubiquitous marine bacterium SAR11. *Nature* **438:** 82-85.
494 Gomelsky M, Klug G. (2002). BLUF: A novel FAD-binding domain involved in sensory
495 transduction in microorganisms. *Trends Biochem Sci* **27:** 497-500.
496 Gómez-Consarnau L, González JM, Coll-Lladó M, Gourdon P, Pascher T, Neutze R *et al*.
497 (2007). Light stimulates growth of proteorhodopsin-containing marine Flavobacteria.
498 *Nature* **445:** 210-213.
499 Gómez-Consarnau L, Akram N, Lindell K, Pedersen A, Neutze R, Milton DL *et al.* (2010).
500 Proteorhodopsin phototrophy promotes survival of marine bacteria during starvation.
501 *PLoS Biol* **8:** e1000358. doi:10.1371/journal.pbio.1000358
502 González JM, Fernández-Gómez B, Fernàndez-Guerra A, Gómez-Consarnau L, Sánchez O,
503 Coll-Lladó M *et al*. (2008). Genome analysis of the proteorhodopsin-containing marine
504 bacterium *Polaribacter* sp. MED152 (Flavobacteria). *Proc Natl Acad Sci USA* **105:**
505 8724-8729.
506 Häse CC, Mekalanos JJ. (1999). Effects of changes in membrane sodium flux on virulence
507 gene expression in *Vibrio cholerae*. *Proc Natl Acad Sci USA* **96:** 3183-3187.
508 Izui K, Matsumura H, Furumoto T, Kai Y. (2004). Phosphoenolpyruvate carboxylase: A new
509 era of structural biology. *Annu Rev Plant Biol* **55:** 69–84.
510 Jitrapakdee S, St. Maurice M, Rayment I, Cleland WW, Wallace JC, Attwood PV. (2008).
511 Structure, mechanism and regulation of pyruvate carboxylase. *Biochem J* **413:** 369–387.
512 Keiler KC. (2008). Biology of *trans*-translation. *Annu Rev Microbiol* **62:** 133-151.
513 Lami R, Cottrell MT, Campbell BJ, Kirchman DL. (2009). Light-dependent growth and
514 proteorhodopsin expression by *Flavobacteria* and SAR11 in experiments with Delaware
515 coastal waters. *Environ Microbiol* **11:** 3201-3209.
516 Martinez A, Bradley AS, Waldbauer JR, Summons RE, DeLong EF. (2007). Proteorhodopsin
517 photosystem gene expression enables photophosphorylation in a heterologous host. *Proc*
518 *Natl Acad Sci USA* **104:** 5590-5595.

519 McCarren J, DeLong EF. (2007). Proteorhodopsin photosystem gene clusters exhibit co-
520 evolutionary trends and shared ancestry among diverse marine microbial phyla. *Environ*
521 *Microbiol* **9:** 846-858.
522 McCarren J, Becker JW, Repeta DJ, Shi Y, Young CR, Malmstrom RR *et al.* (2010).
523 Microbial community transcriptomes reveal microbes and metabolic pathways associated
524 with dissolved organic matter turnover in the sea. *Proc Natl Acad Sci USA* **107:** 16420-
525 16427.
526 Moore SD, Sauer RT. (2007). The tmRNA System for translational surveillance and
527 ribosome rescue. *Annu Rev Biochem* **76:** 101-124.
528 Moran MA, Miller WL. (2007). Resourceful heterotrophs make the most of light in the
529 coastal ocean. *Nat Rev Microbiol* **5:** 792-800.
530 Reich M, Liefeld T, Gould J, Lerner J, Tamayo P, Mesirov JP. (2006). GenePattern 2.0. *Nat*
531 *Genet* **38:** 500-501.
532 Sabehi G, Loy A, Jung KH, Partha R, Spudich JL, Isaacson T *et al.* (2005). New insights into
533 metabolic properties of marine bacteria encoding proteorhodopsins. *PLoS Biol* **3:** e273.
534 Shi Y, Tyson GW, DeLong EF. (2009). Metatranscriptomics reveals unique microbial small
535 RNAs in the ocean's water column. *Nature* **459:** 266–269.
536 Spudich JL, Jung KH. (2005). Microbial rhodopsin: phylogenetic and functional diversity. In:
537 Briggs WR, Spudich JL (eds). *Handbook of Photosensory Receptors*. Wiley-VCH Verlag
538 GmbH & Co. KGaA: Weinheim, Germany. pp 1-24.
539 Stewart FJ, Ottesen EA, DeLong EF. (2010). Development and quantitative analyses of a
540 universal rRNA-subtraction protocol for microbial metatranscriptomics. *ISME J* **4:** 896-
541 907.
542 Stingl U, Desiderio RA, Cho J-C, Vergin KL, Giovannoni SJ. (2007). The SAR92 clade: an
543 abundant coastal clade of culturable marine bacteria possessing proteorhodopsin. *Appl*
544 *Environ Microbiol* **73:** 2290-2296.
545 Storey JD, Tibshirani R. (2003). Statistical significance for genomewide studies. *Proc Natl*
546 *Acad Sci USA* **100:** 9440–9445.
547 Taylor BL, Zhulin IB. (1999). PAS domains: internal sensors of oxygen, redox potential, and
548 light. *Microbiol Mol Biol Rev* **63:** 479-506.
549 Tokuda H, Unemoto T. (1982). Characterization of the respiration-dependent Na^+ pump in
550 the marine bacterium *Vibrio alginolyticus*. *J Biol Chem* **257:** 10007-10014.
551 Walter JM, Greenfield D, Bustamante C, Liphardt J. (2007). Light-powering *Escherichia coli*
552 with proteorhodopsin. *Proc Natl Acad Sci USA* **104:** 2408-2412.

Figure Legends

Figure 1 Growth of MED134 incubated in the light or in the dark. MED134 was grown in unenriched ASW (0.05 mM C) (**a**), in ASW enriched to 0.14 mM C (**b**), and in ASW enriched to 0.39 mM C (**c**). The cultures were incubated under continuous white light (○), or in the darkness (●). Errors bars denote standard deviation for triplicate.

Figure 2 Inventory of RNAs from cultures in the microbial transcriptomic datasets. MED 134 was first incubated in ASW enriched to 0.14 mM C in the dark for first 2 days (D2). Then culture was split in two flasks, with one incubated in the light (L2), and the other in the dark (D4), for 2 more days. Numbers in the pie charts represent the percentage of total cDNA reads in each transcriptomic dataset. [a]Subtraction of 16S and 23S rRNAs were performed after total RNA extraction.

Figure 3 Transcriptomic analyses of proteorhodopsin and retinal biosynthetic genes. (**a**) Retinal biosynthetic pathway. The colors indicate the L2/D4 ratio of retinal biosynthetic enzymes. The ratio was calculated based on abundance of reads for each specific gene, normalized by the total number of protein-encoding reads for each sample. (**b**) Cluster analysis of the relative abundance of PR and retinal biosynthetic enzymes. Hierarchical clustering was performed based on the number of cDNA reads, normalized to the total number of protein-encoding cDNAs in each sample, using a Pearson correlation. The heat map shows relative difference of transcript abundance in each sample (red indicates high Pearson correlation; white indicates intermediate; blue indicates low). The numbers of cDNA read are summarized in Table 1. IPP, isopentenyl pyrophosphate; DMAPP, dimethylallyl pyrophosphate; FPP, farnesyl pyrophosphate; GGPP, geranylgeranyl pyrophosphate; MPTA, 2-(4-methylphenoxy)triethylamine hydrochloride.

578

579 **Figure 4** Colony image and growth of MED134 in culture experiments with a specific
580 inhibitor of lycopene cyclization, 2-(4-methylphenoxy)triethylamine hydrochloride (MPTA).
581 (**a** and **b**) Colony morphology of MED134 on Marine Agar 2216 (Difco) plate amended with
582 MPTA (**a**) and without MPTA (**b**). (**c** and **d**) Microbial cell density in ASW enriched with
583 peptone and yeast extracts (0.14 mM C) and amended with MPTA in culture exposed to light
584 (△) and in the dark (▲), and in the ASW amended without MPTA in culture exposed to
585 light (○) and in the dark (●). Bacterial cells were counted by epifluorescence microscopy (**c**)
586 and plate count method (**d**). cfu, colony-forming unit.

587

588 **Figure 5** Growth of MED134 in cultures incubated with 2-n-heptyl-4-hydroxyquinoline N-
589 oxide (HQNO), a specific inhibitor of Na^+-translocating NADH-quinone oxioreductase
590 (NQR). MED134 were grown in ASW enriched with DL-alanine (0.7 mM C). Cultures
591 were incubated in the ASW amended with HQNO in light (△) or dark (▲) and in the ASW
592 without HQNO in light (○) or dark (●). Bacterial cell densities were determined by
593 epifluorescence microscopy (**a**) and plate count method (**b**). cfu, colony-forming unit.

594

595 **Figure 6** Model of light-stimulated transcriptional responses in MED134. Proton pumping
596 processes and retinal biosynthetic pathway are shown in left, whereas central metabolic
597 pathways, such as glycolysis, pentose phosphate cycle, and TCA cycle, are in right. The
598 color allows and membrane proteins indicate the value of L2/D4 ratio. The ratio is calculated
599 based on abundance of reads for each gene normalized by total number of protein-encoding
600 reads for each sample. PR, proteorhodopsin; PP, pyrophosphatase; NQR, Na^+-translocating
601 NADH-quinone oxidoreductase; SDH, succinate dehydrogenase; Cyt, cytochrome oxidase;
602 NHA, Na^+/H^+ antiporter.

Figure 1

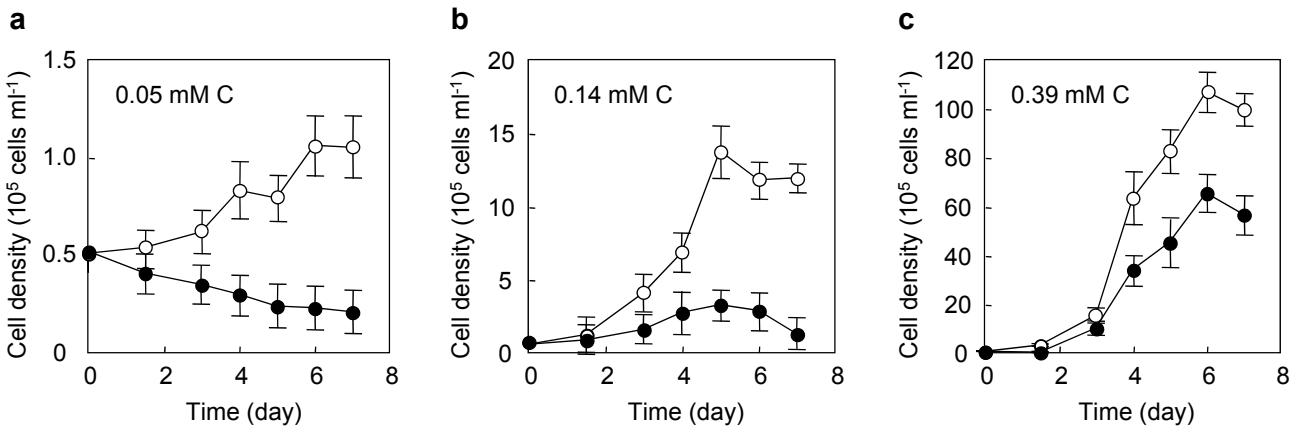
a
0.05 mM C
Cell density (10^5 cells ml^{-1})
Time (day)
b
0.14 mM C
Cell density (10^5 cells ml^{-1})
Time (day)
c
0.39 mM C
Cell density (10^5 cells ml^{-1})
Time (day)

Figure 2

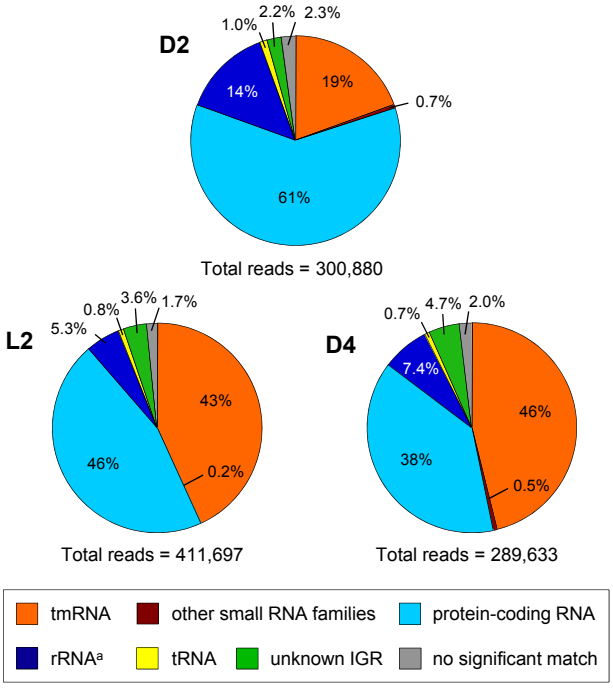
D2
1.0%
2.2%
2.3%
19%
0.7%
14%
61%
Total reads = 300,880
L2
0.8%
3.6%
1.7%
5.3%
43%
46%
0.2%
Total reads = 411,697
D4
0.7%
4.7%
2.0%
7.4%
46%
38%
0.5%
Total reads = 289,633
tmRNA
other small RNA families
protein-coding RNA
rRNA[a]
tRNA
unknown IGR
no significant match

Figure 3

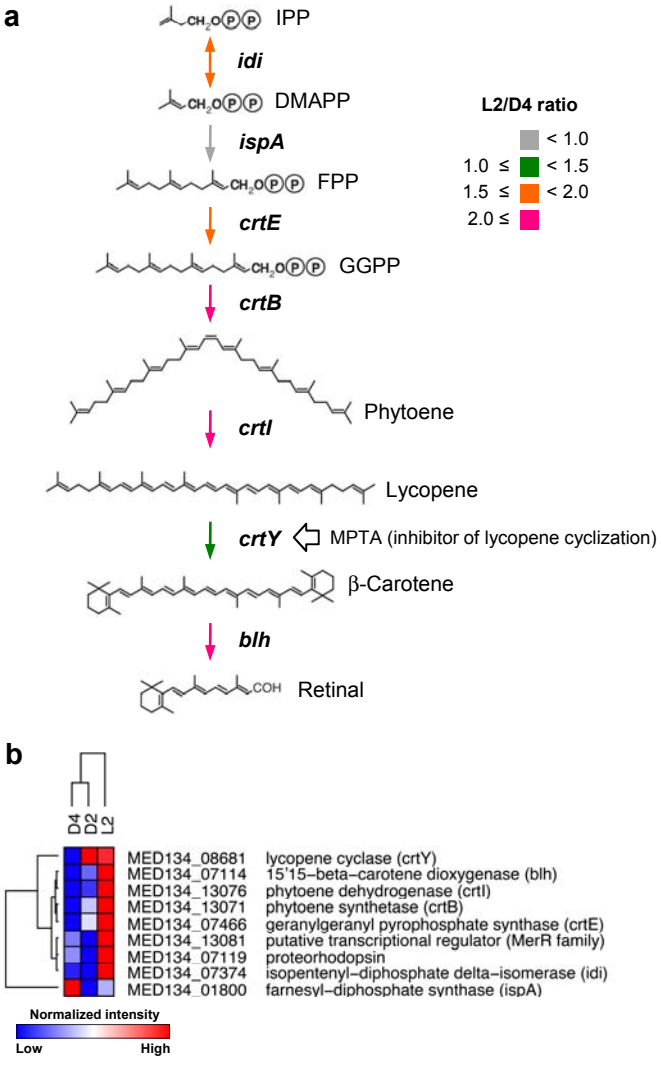
a
IPP
idi
DMAPP
ispA
FPP
crtE
GGPP
crtB
Phytoene
crtI
Lycopene
crtY
MPTA (inhibitor of lycopene cyclization)
β-Carotene
blh
Retinal
L2/D4 ratio
< 1.0
1.0 ≤ < 1.5
1.5 ≤ < 2.0
2.0 ≤
b
D4
D2
L2
MED134_08681 lycopene cyclase (crtY)
MED134_07114 15'15–beta–carotene dioxygenase (blh)
MED134_13076 phytoene dehydrogenase (crtI)
MED134_13071 phytoene synthetase (crtB)
MED134_07466 geranylgeranyl pyrophosphate synthase (crtE)
MED134_13081 putative transcriptional regulator (MerR family)
MED134_07119 proteorhodopsin
MED134_07374 isopentenyl–diphosphate delta–isomerase (idi)
MED134_01800 farnesyl–diphosphate synthase (ispA)
Normalized intensity
Low
High

Figure 4

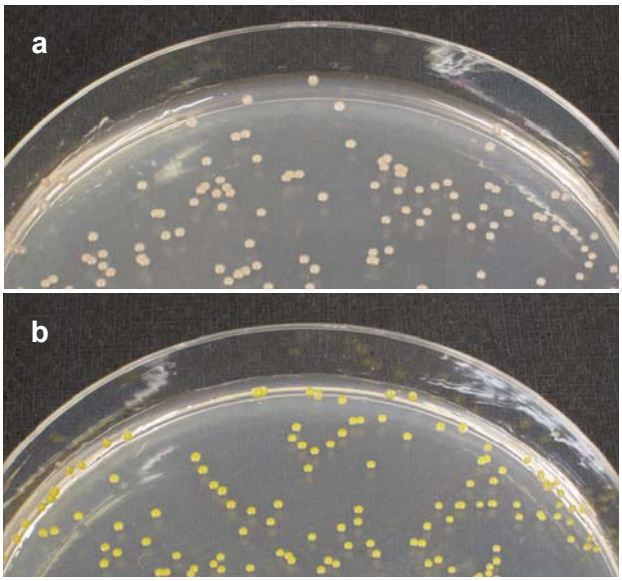
a
b

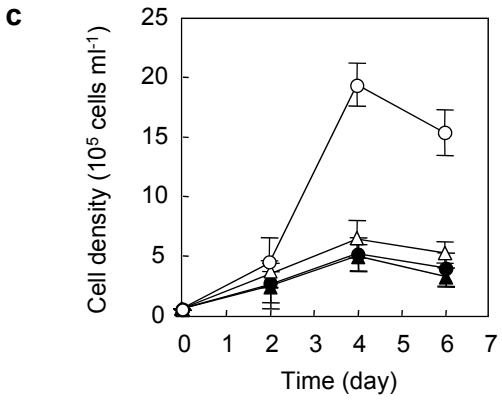
c
Cell density (10^5 cells ml^-1)
25
20
15
10
5
0
0 1 2 3 4 5 6 7
Time (day)

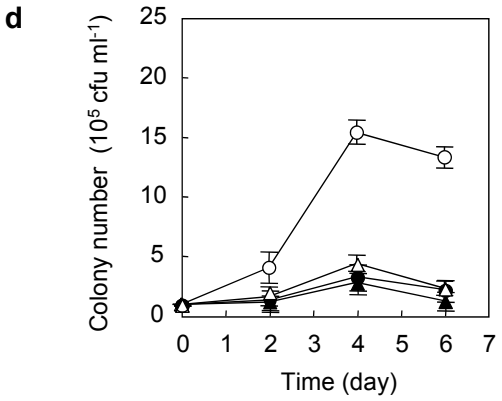
d
Colony number (10^5 cfu ml^-1)
25
20
15
10
5
0
0 1 2 3 4 5 6 7
Time (day)

Figure 5

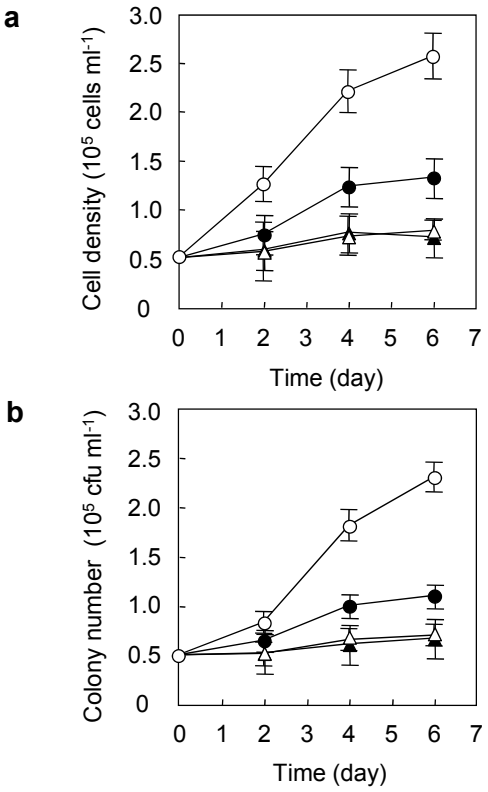
a
Cell density (10^5 cells ml^{-1})
3.0
2.5
2.0
1.5
1.0
0.5
0
0 1 2 3 4 5 6 7
Time (day)
b
Colony number (10^5 cfu ml^{-1})
3.0
2.5
2.0
1.5
1.0
0.5
0
0 1 2 3 4 5 6 7
Time (day)

Figure 6

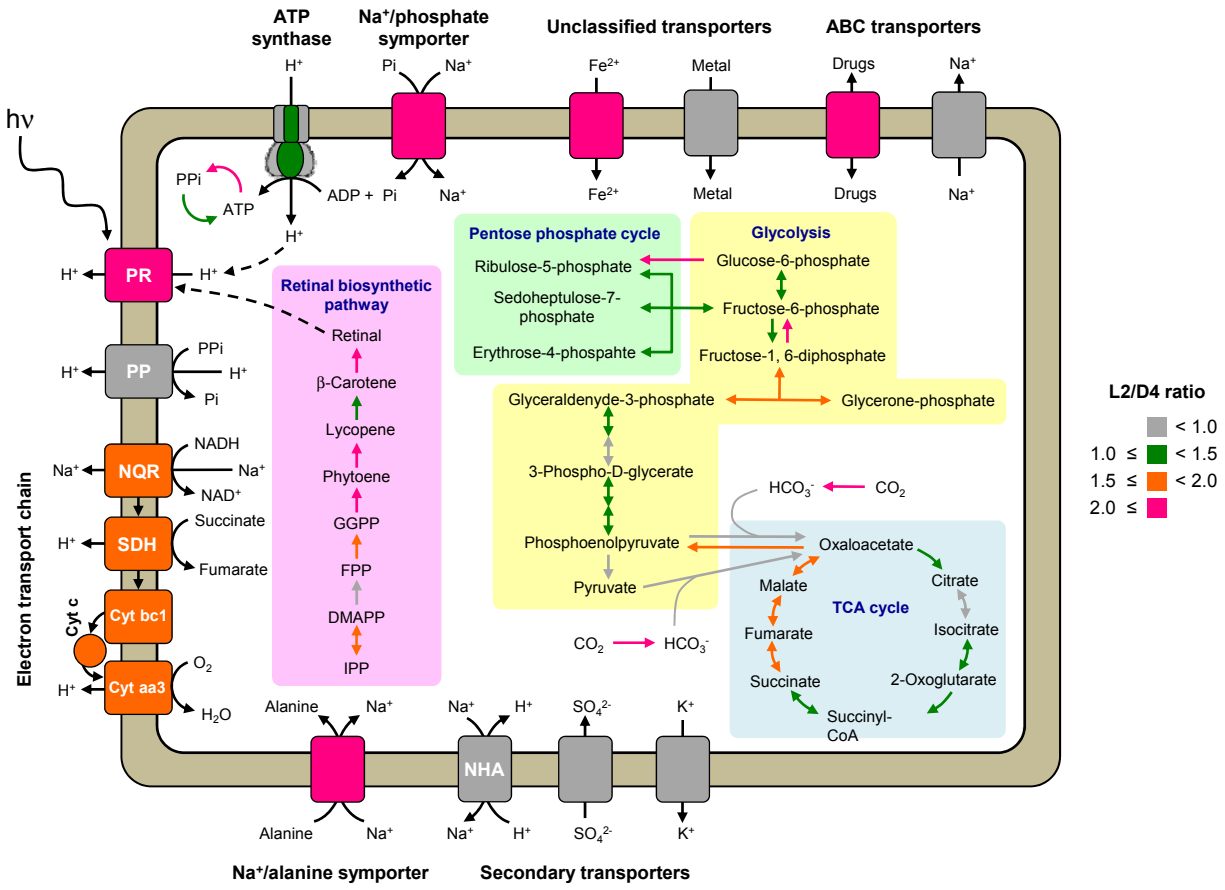
ATP synthase
Na+/phosphate symporter
Unclassified transporters
ABC transporters
hν
PR
PP
NQR
SDH
Cyt bc1
Cyt aa3
Cyt c
Electron transport chain
Retinal biosynthetic pathway
Retinal
β-Carotene
Lycopene
Phytoene
GGPP
FPP
DMAPP
IPP
Pentose phosphate cycle
Ribulose-5-phosphate
Sedoheptulose-7-phosphate
Erythrose-4-phospahte
Glycolysis
Glucose-6-phosphate
Fructose-6-phosphate
Fructose-1, 6-diphosphate
Glyceraldenyde-3-phosphate
Glycerone-phosphate
3-Phospho-D-glycerate
Phosphoenolpyruvate
Pyruvate
TCA cycle
Oxaloacetate
Citrate
Isocitrate
2-Oxoglutarate
Succinyl-CoA
Succinate
Fumarate
Malate
NHA
Na+/alanine symporter
Secondary transporters
L2/D4 ratio
< 1.0
1.0 ≤ < 1.5
1.5 ≤ < 2.0
2.0 ≤

Table 1 Read number and L2/D4 ratio of protein-encoding cDNA that plays a crital role in light-stimulated growth

Name	*Locus tag*	*Size (aa)*	*Read number*			*L2/D4 ratio*	q-*value*
			D2	*L2*	*D4*		
Opsin							
Proteorhodopsin	MED134_07119	247	1	33	5	3.92	**0.0129**
Retinal biosynthetic enzymes							
Isopentenyl-diphosphate δ-isomerase (*idi*)	MED134_07374	172	17	36	11	1.94	0.1568
Farnesyl-diphosphate synthase (*ispA*)	MED134_01800	325	27	30	21	0.85	0.7416
Geranylgeranyl pyrophosphate synthase (*crtE*)	MED134_07466	324	53	77	23	1.99	**0.0160**
Phytoene synthetase (*crtB*)	MED134_13071	279	20	34	8	2.53	0.0660
Phytoene dehydrogenase (*crtI*)	MED134_13076	486	37	86	20	2.56	**0.0005**
Lycopene cyclase (*crtY*)	MED134_08681	403	10	10	4	1.49	0.7585
15,15'-β-carotene dioxygenase (*blh*)	MED134_07114	287	2	4	1	2.38	0.8027
Transcriptional regulator, MerR family	MED134_13081	309	9	22	7	1.87	0.3648
Transporters							
Na^+/alanine & glycine symporter	MED134_02355	561	90	84	27	1.85	**0.0241**
Na^+/alanine & glycine symporter	MED134_14567	509	64	52	13	2.38	**0.0243**
Na^+/phosphate symporter	MED134_11180	745	81	64	15	2.54	**0.0049**
Electron transport chain							
Na^+-translocating NADH quinone oxidoreductase (*nqrA*)	MED134_00295	448	713	1308	518	1.50	**<0.0001**
Na^+-translocating NADH quinone oxidoreductase (*nqrB*)	MED134_00300	400	406	753	268	1.67	**<0.0001**
Na^+-translocating NADH quinone oxidoreductase (*nqrC*)	MED134_00305	248	101	181	56	1.92	**0.0001**
Na^+-translocating NADH quinone oxidoreductase (*nqrD*)	MED134_00310	215	93	147	34	2.57	**<0.0001**
Na^+-translocating NADH quinone oxidoreductase (*nqrE*)	MED134_00315	228	73	97	38	1.52	0.1115
Na^+-translocating NADH quinone oxidoreductase (*nqrF*)	MED134_00320	435	250	485	165	1.75	**<0.0001**

Statistical significance between light and dark cultures was measured based on *q*-value (false discovery rate method). The features with *q*-values ≤0.05 are significant (Storey and Tibshirani, 2003), which are underline and in bold.

Table 2 Read number and L2/D4 ratio of cDNA encoding domains and peotides with a role in light absorption and response

Name	*Locus tag*	*Size (aa)*	*Read number*			*L2/D4 ratio*	q-*value*
			D2	*L2*	*D4*		
Bacterial cryptochrome, DASH family	MED134_10201	432	9	29	5	3.45	**0.0341**
DNA photolyase/cryptochrome, (6-4) photolyase family	MED134_10206	511	5	22	2	6.54	**0.0149**
DNA photolyase/cryptochrome, (6-4) photolyase family	MED134_10211	494	3	24	3	4.75	**0.0244**
DNA photolyase/cryptochrome, class I photolyase	MED134_14266	436	37	38	12	1.88	0.1700
PAS domain	MED134_02435	1200	87	66	37	1.06	0.9091
GAF domain	MED134_01075	151	53	56	37	0.90	0.8120
Phytochrome region	MED134_02440	749	27	32	9	2.11	0.1574
BLUF domain	MED134_02460	338	38	18	11	0.97	0.9371
Multi-sensor hybrid His kinase	MED134_01400	741	109	116	37	1.86	**0.0058**
Two-component system sensor His kinase	MED134_07876	182	11	12	12	0.59	0.4031
Sensory transduction His kinase	MED134_10396	163	3	123	4	18.3	**<0.0001**
Sensory transduction His kinase	MED134_06794	657	48	54	31	1.04	0.9371
Sensory transduction His kinase	MED134_07881	470	42	29	15	1.15	0.8630

Statistical significance between light and dark cultures was measured based on *q*-value (false discovery rate method). The features with *q*-values ≤0.05 are significant (Storey and Tibshirani, 2003), which are underline and in bold.